Water splitting under visible light using aerogel prepared strontium titanate ($SrTiO_3$) nanomaterials doped with ruthenium and rhodium metals

Yenting Kuo and Kenneth J. Klabunde

Water Splitting under Visible Light using Aerogel Prepared Strontium Titanate ($SrTiO_3$) Nanomaterials Doped with Ruthenium and Rhodium Metals.

Yenting Kuo, and Kenneth J. Klabunde*

Department of Chemistry, Kansas State University, KS, 66506, USA

Corresponding author: - Fax +1-785-532-6666

Email address: kenjk@ksu.edu (K. J. Klabunde)

Abstract

Nanostructured strontium titanate visible-light-driven photocatalysts containing rhodium and ruthenium were synthesized by a modified aerogel synthesis using ruthenium chloride and rhodium nitrate as dopants precursors, and titanium isopropoxide and strontium metal for the metal sources. The well-defined crystalline $SrTiO_3$ structure was confirmed by X-ray diffraction (XRD). After calcination at 500 °C, diffuse reflectance spectroscopy shows the increase of light absorption at 370 nm due to the presence of Rh^{3+}; however an increase of calcination temperature to 600 °C led to a decrease in intensity, probably due to loss of surface area. An increase in rhodium doping amount also led to an increase in absorption at 370 nm; however, they higher amounts of dopant lowered photocatalytic activity. The modified aerogel synthesis allows greatly enhanced H_2 production performance from an aqueous methanol solution under visible light irradiation, compared with lower surface area conventional materials. We believe this enhanced activity is due to higher surface areas while still yielding high quality nanocrystalline materials. Furthermore, the surface properties of these nanocrystalline aerogel materials are different, as exhibited by higher activities in alkaline solutions, while conventional materials (via high temperature solid-state synthesis methods) only exhibit reasonable hydrogen production in acidic solutions. Moreover, an aerogel synthesis approach gives the possibility of thin-film formation and ease of incorporation for practical solar devices.

1. Introduction

Many photocatalysts have been reported for water splitting under UV-Vis light. However, visible-light-driven photocatalysts are of more interest because sun-light possesses a larger portion of visible light. Fewer materials for water splitting under visible light have been reported. Domen and coworkers have reported GaN-ZnO and $GeZnN_2$-ZnO solid solutions for overall water splitting under visible light.[11, 12, 10] However, these oxy(nitride) photocatalysts need the assistance of co-catalysts such as Cr_2O_3-Rh_2O_3 to be active. On the other hand, two-step photocatalysis systems for overall water splitting mimicking photosynthesis in green plants have been broadly studied. These Z-scheme photocatalysis systems are composed of two photocatalysts, which generate H_2 and O_2 by different catalysts along with a reversible redox couple. The redox couple acts an electron mediator to transfer electrons from the O_2 production photocatalyst to the H_2 production photocatalyst. Fujihara et al. achieved overall water splitting using a system consisting of Pt/TiO_2-Br and TiO_2-Fe^{3+} components, but it only worked under UV light irradiation.[5] Some other visible-light-driven systems also have been reported.[16, 1, 6] Sayama et al. and Abe et al. reported Z-scheme photocatalysis systems using an IO^{3-} /I^- redox couple as an electron mediator.[16, 1] Moreover, Kudo et al. observed visible-light-driven Z-scheme photocatalysis systems using Pt/$SrTiO_3$:Rh for H_2 evolution,[8] $BiVO_4$,[9] Bi_2MoO_6,[17] and WO_3[2] for O_2 evolution along with Fe^{3+}/Fe^{2+} couple as a electron mediator.[6, 7] However, Pt co-catalyst not only assists water splitting reactions but also back-recombination reactions, such as water formation from evolved H_2 and O_2. In contrast to Pt, a Ru co-catalyst is an effective cocatalyst that does not enhance the back reaction.[14] Therefore, Ru may be a better choice than Pt to be the reaction sites for H_2 generation on the surface of composites as a co-catalyst.

$SrTiO_3$:Rh is a proven photocatalyst with high activity for H_2 evolution in methanol-water solution under visible light.[8] The unique character of doped Rh has reversible oxidation states (+3, +4, etc.) in $SrTiO_3$. Therefore, the $SrTiO_3$:Rh photocatalyst is activated by the help of reduction of Rh(IV) to Rh(III) during H_2 evolution in an aqueous methanol solution under visible light irradiation.[8]

In this study, we report that crystalline $SrTiO_3$:Rh can be prepared by a modified aerogel procedure.[3] The synthesis of mixed metal oxides by sol-gel or aerogel methods can be achieved by the co-gelation of metal precursors to form single-phase nanosized strontium titanate. However, the product often consists of two separate oxide phases. In this research, the mixed alkoxide route through the mixing of two metal alkoxides results in a better gelation and higher purity of final product. The supercritical drying procedure allows higher surface areas and uniform pore structure, and helps to prevent strontium oxides from forming a carbonate phase by reacting with CO_2 in air during hydrolysis. The influence of solvent on the aerogel process also has been previously studied in our research group.[18, 4, 3] It was found that two different polarities of a mixed solvent system can help to control the hydrolysis of the aerogel resulting in a higher surface area. The added hydrophobic solvent may reduce tension in gel pores and further prevent sintering.[18] Therefore, we used mixed ethanol-toluene as a solvent to perform the aerogel synthesis.

2. Materials and methods

All procedures were performed under argon, because strontium metal is sensitive to water and oxygen. All autoclave treatments for supercritical drying were performed on a Parr 4843

instrument. SrCO (≥ 99.9% trace metals basis), TiO_2 (nanopowder, ~21 nm particle size, ≥ 99.5% trace metals basis), Rh_2O_3 (powder, 99.8%), $RuCl_3 \cdot nH_2O$ (99.98% trace metals basis), Titanium (IV) isopropoxide (97%), absolute ethanol (200 proof), calcium hydrate (powder, 99.99% trace metals basis), toluene strontium metal (99% dendritic pieces), and Rhodium(III) nitrate solution ~10 % (w/w) (Rh in > 5 wt. % HNO_3) were used as received.

Synthesis of strontium titanium oxide doped with rhodium was carried out by a conventional solid-state reaction.[14, 8] The starting materials, $SrCO_3$, TiO_2 and Rh_2O_3 were mixed in a mortar according to the ratio Sr/Ti/Rh = 1.07:0.99:0.01. The mixture was calcined at 1273 K for 10 h in air. Ru (1.0 wt %) co-catalyst (working as active sites for H_2 evolution) were loaded on the photocatalysts by photodeposition from aqueous methanol solutions (10 vol%) containing $RuCl_3 \cdot nH_2O$.[14] The cocatalyst-loaded photocatalysts were collected by filtration and washed with water.

Synthesis of higher surface area strontium titanate was carried out by a modified aerogel procedure (figure 1) described in our group's previous publication.[3] However, in the current applications Rh doping was carried out. Different mole ratios of Rh (1-1.75 %) were added into system after alkoxide solutions were mixed. Later, the resulting $SrTiO_3$:Rh powders were annealed in air at different temperatures to remove the residual solvent. Ru co-catalysts were loaded on photocatalysts by photodeposition from aqueous methanol solutions (10 vol%) containing $RuCl_3 \cdot nH_2O$.[14] The cocatalyst-loaded photocatalysts were collected by filtration and washed with water.

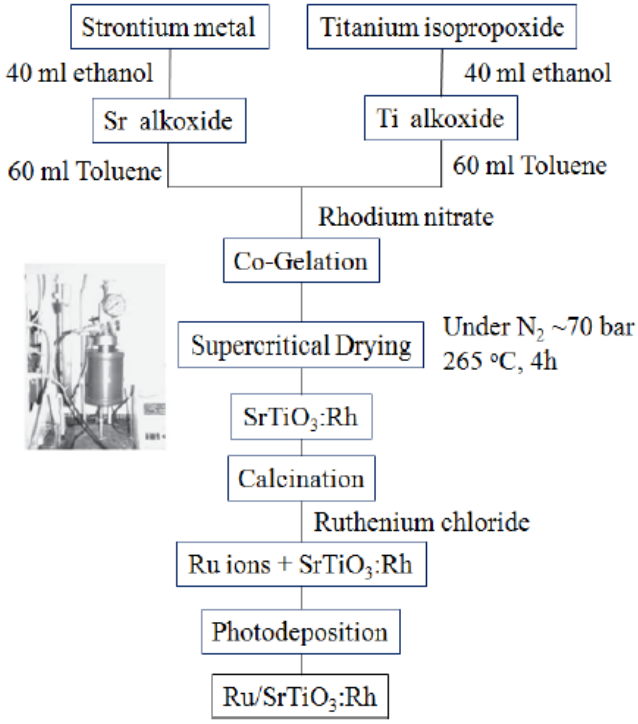

Figure 1. Modified aerogel procedure from alkoxides for Ru/$SrTiO_3$:Rh synthesis.

Photocatalytic Reactions were carried out in a glass-enclosed reaction chamber connected to a gas circulation and evacuation system with a quartz inner irradiation-type reaction vessel. The reaction was performed in a 345 ml 10 % ethanol solution and containing 0.3 g of the $SrTiO_3$:Rh sample. The pHs of solutions were adjusted by NaOH for aerogel synthesis samples. The test condition for conventional solid-state synthesis samples was followed exactly as given by Kudo etc.[8, 14] The reactant solution was evacuated and filled with argon three times to remove air completely, followed by irradiation under a 450 W high-pressure Hg lamp via a quartz tube that was filled with 2 M $NaNO_2$ aqueous solution for visible light studies. H_2 production was monitored during the reaction with an online GC system (GOMAC model) employing a Supelco molecular 80/100 sieve 5A column with Ar as the carrier gas and a thermal conductivity detector (TCD).

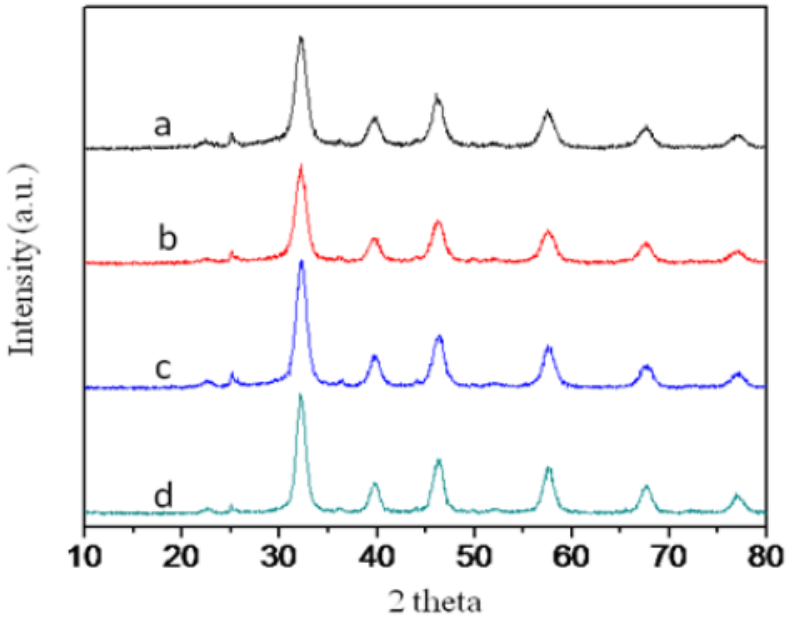

Figure 2. Powder XRD patterns of $SrTiO_3$:Rh calcined in air at different temperatures. (a) as synthesized (b) 300 ℃ (c) 400 ℃ (d) 500 ℃

Table 1. Characteristic properties of $SrTiO_3$:Rh (1 mole %) calcined in air at different temperatures.

Calcination temperature (℃)	Average crystallite size (nm)	Surface Area (m^2/g)	Total pore volume (cm^2/g)	Average pore size (nm)
n/a	5	130	0.76	15.7
300	5.8	106	0.54	15.7
400	6	111	0.57	15.7
500	6.8	78.4	0.52	15.7

3. Results and discussion

3.1. Strontium titanates calcination at different temperatures.

$SrTiO_3$:Rh samples have been synthesized by the aerogel method and calcined at different temperatures. Figure 2 shows the XRD patterns of $SrTiO_3$:Rh treated previously at different calcination temperatures. The XRD patterns confirm the well-defined crystalline $SrTiO_3$ structure. These samples do not require high-temperature treatments to initiate a phase transition from amorphous to crystalline. The Rhodium could not be observed in the XRD pattern, because it was loaded at only 1 mole %. The crystallite sizes of different calcination temperatures are shown in table 1. The highest surface area that we obtained is 130 m^2/g, which is much higher than that achieved by solid-state or hydrothermal synthesis methods. Table 1 shows the higher calcination temperature, the larger the crystallite size obtained from the XRD pattern. This shows that the higher calcination temperature can improve the crystal structure and reduce the defects by atom rearrangement. The better crystalline nature may result in a higher water splitting activity. However, the surface area and the total pore volume decrease when a higher calcination temperature was applied. Surface area is also very important for a catalyst. A large surface can increase the water-catalyst interface resulting in a better activity. Therefore, the highest catalytic activity achievement must be balanced at a certain point between crystallinity and surface area. Moreover, calcination is a necessary treatment for most catalysts. It can remove the residues of solvent or other organic agents, which were used during the synthesis. The different calcination temperatures for the resulting samples also have been tested, which shows that 500 ^oC is the turning point of calcination temperature influence between crystallinity, surface area and solvent residue removal, (note the dramatic decrease of surface area, table 1). The water splitting reactions were conducted in a 10 vol % methanol solution after further doping with Ru as a co-

catalyst. Ru is used as a co-catalyst for the hydrogen production. It can be homogeneously doped by the photodeposition method.

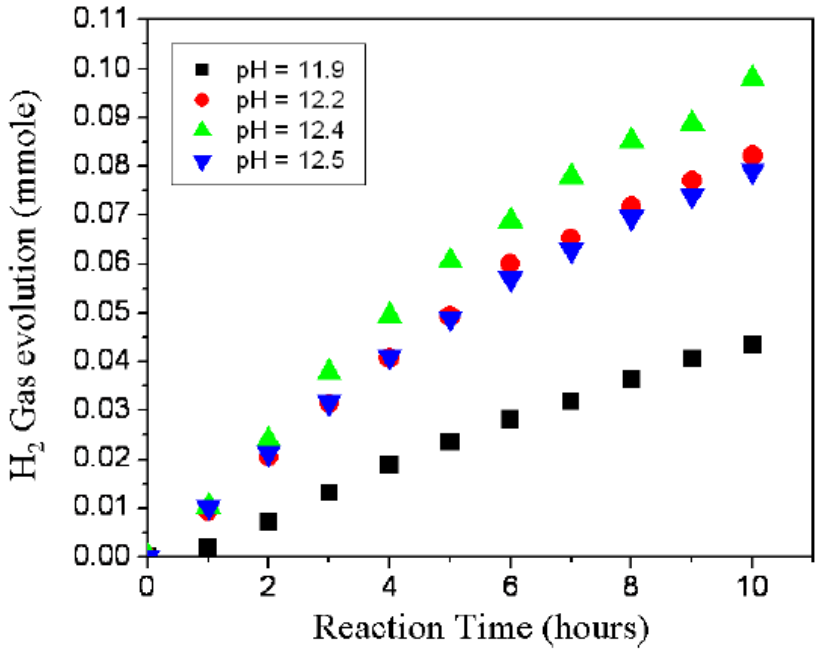

Figure 3. Dependence of H_2 evolution activity of $SrTiO_3$:Rh (1.5 wt% Ru, 1 mole% Rh, cal. 550 °C) at different pHs under visible light in 10 vol% methanol-water solution.

3.2. H_2 generation of strontium titanate at different pHs.

Aerogel synthesis $SrTiO_3$:Rh samples have a very different character than the solid-state synthesis samples. Aerogel synthesis samples have higher hydrogen production activities under basic (alkaline) conditions compared with solid-state synthesis samples, which have higher activity under acidic conditions. Figure 3 shows the relativity activities of H_2 production of aerogel $SrTiO_3$:Rh (1.5 wt% Ru, 1mole % Rh, calcination temperature 550 ^oC) under visible light in 10 vol % methanol solution at different pHs. The result shows that the H_2 production is very sensitive to solution pH and pH = 12.4 is the best condition for the aerogel synthesis samples. Moreover, Rabuffetti etc el. showed by chemisorption of atmospheric CO_2 and pyridine,

as probes of acid and base sites, that the differences in surface acidity between samples of $SrTiO_3$ synthesized using different approaches are rather slight with a mixture of SrO-based and TiO-based terminations.[13] On the other hand, their results showed that surface atomic structure of $SrTiO_3$ depends strongly on the synthetic method with regard to the reactive adsorption of atmospheric CO_2, which varied significantly between samples. These results suggest that these aerogel materials possess more nucleophilic O^{2-} surface centers. Perhaps the preferred higher pH reaction conditions help preserve those reaction O^{2-} sites, that seem to be important in the overall water splitting mechanism.

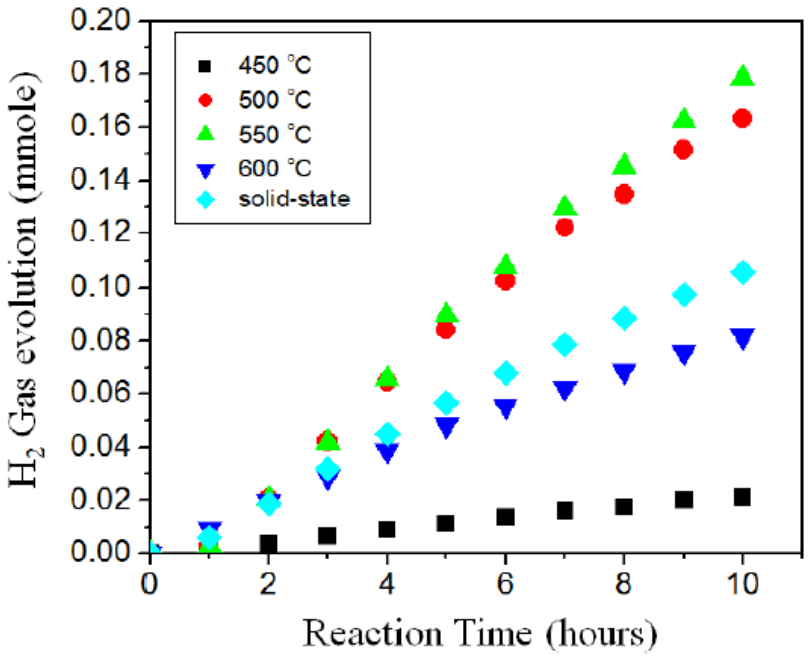

Figure 4. Dependence of H_2 evolution activity of $SrTiO_3$:Rh (1.5 wt% Ru, 1 mole% Rh) upon different calcination temperatures under visible light in 10 vol % methanol-water solution.

3.3. Dependence of H_2 evolution activity of aerogel Ru/$SrTiO_3$:Rh on different calcination temperatures.

$SrTiO_3$:Rh samples with different calcination temperatures show a variation in H_2 evolution activity (figure 4) (pH = 12.4, adjusted by NaOH under visible light, with a conventional solid-state synthesized sample for comparison). The results show that a calcination temperature of 550 ^oC has the best activity. The calcination temperatures strongly affected the nanoparticle surface condition. Figure 5 shows the diffuse reflectance spectra of Rh-doped aerogel $SrTiO_3$ (1.5 wt% Ru, 1.25 mole% Rh) with different calcination temperatures. The decrease of absorption between 500 nm to 800 nm when calcination temperatures were increased from 450 ^oC to 500 ^oC may be due to loss of organic contaminants. Indeed, figure 5c corresponds to the most active catalysts with calcination at 550 ^oC. The absorption band in the visible region at 420 nm is contributed to Rh^{3+}.[15] We believe that Rh^{3+} is an important visible light chromophore, and is present even up to 550 ^oC. Thus, it is likely that the Rh^{3+} sites are important for light induced exciton formation.

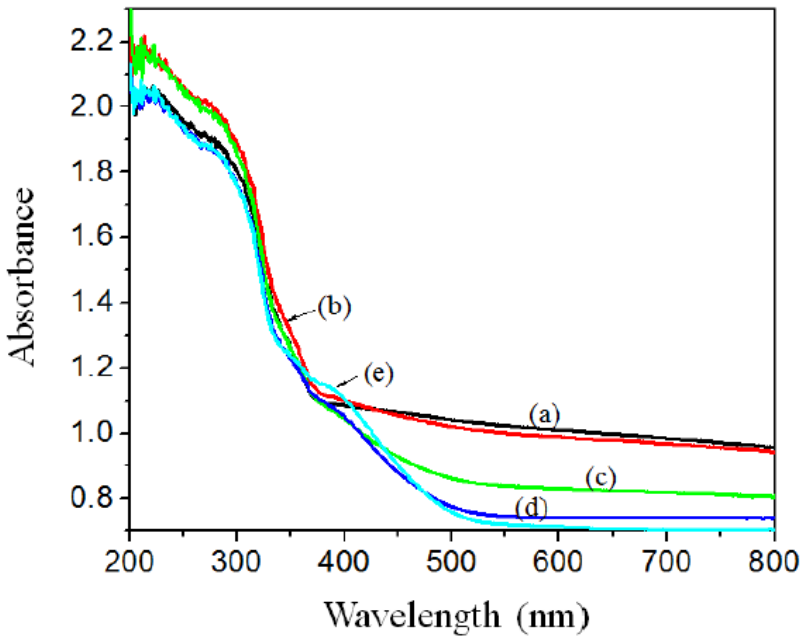

Figure 5. Diffuse reflectance spectra of Rh-doped aerogel $SrTiO_3$ (1.5 wt% Ru, 1.25 mole% Rh) from different calcination temperatures (a) 450 °C (b) 500 °C (c) 550 °C (d) 600 °C (e) 650 °C.

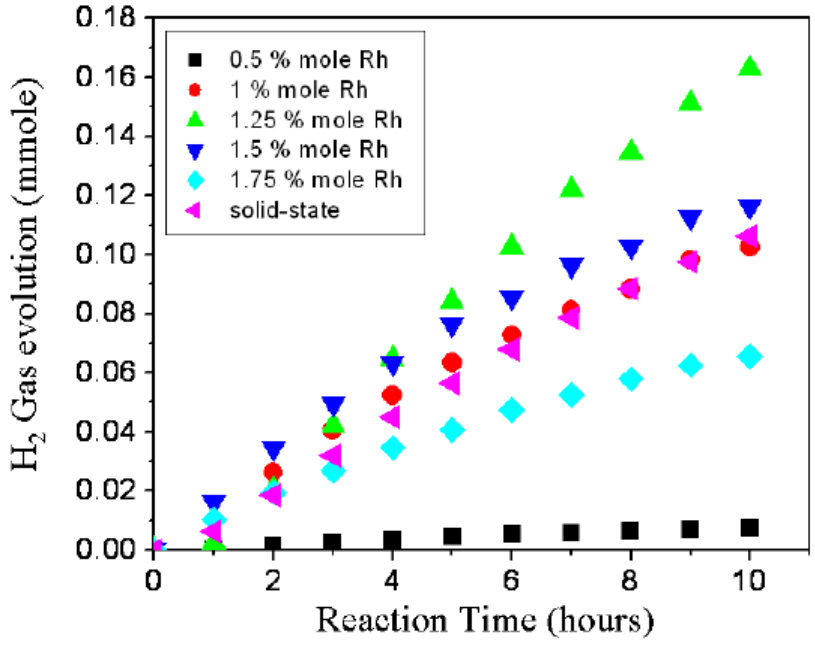

Figure 6. Dependence of H_2 evolution activity of Rh-doped aerogel $SrTiO_3$ (1.5 wt% Ru, cal. 500 °C) at different doping amounts in 10 vol % methanol-water solution (pH = 12.4, adjusted by NaOH) under visible light.

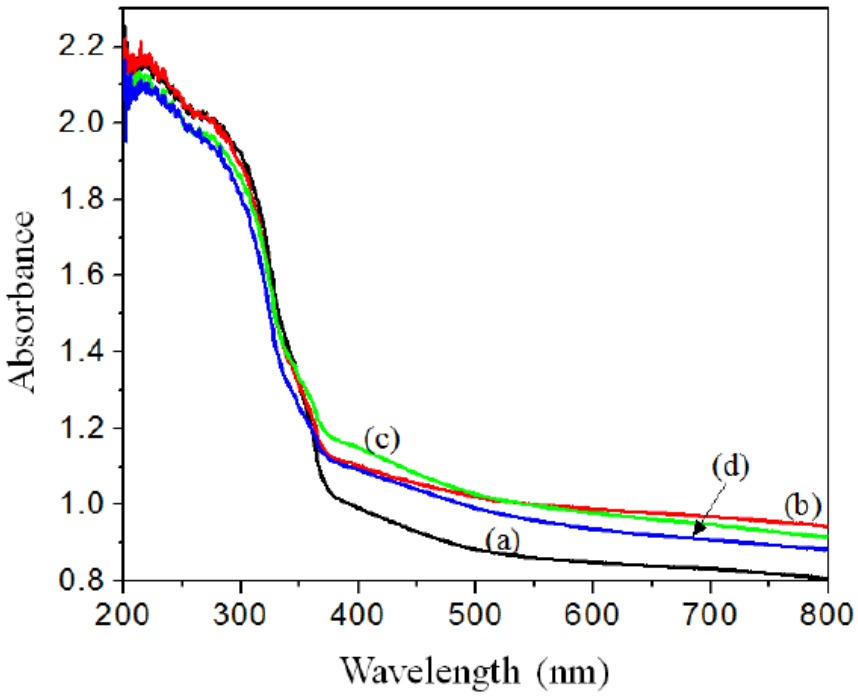

Figure 7. Diffuse reflectance spectra of Rh-doped aerogel $SrTiO_3$ (1.5 wt% Ru, cal. 500 °C) from different doping amounts (a) 1 mole% (b) 1.25 mole% (c) 1.5 mole% (d) 1.75 mole%.

3.4. Dependence of H_2 evolution activity of aerogel Ru/$SrTiO_3$:Rh on different Rh doping amounts.

$SrTiO_3$:Rh samples with different amounts of Rh have been synthesized by the modified aerogel method. Figure 6 shows dependence of H_2 evolution activity of Rh-doped aerogel $SrTiO_3$ (1.5 wt% Ru, cal. 500 ^oC) upon the different doping amount in 10 vol % methanol solution (pH = 12.4, adjusted by NaOH) under visible light along with a conventional solid-state synthesized sample for comparison. The optimal doping amount is Ru/$SrTiO_3$:Rh(1.25 mole % Rh) (figure 6). The highest hydrogen production can generate ~54 % more H_2 gas than a solid-state synthesis sample in 10 hours. Figure 7 shows the diffuse reflectance spectra of Rh-doped aerogel $SrTiO_3$ (1.5 wt% Ru, cal. 500 ^oC) with different doping amounts. The highest visible light absorption starting from 520 nm was found for samples with higher loading than 1.0 mole% of Rh, and these loadings are optional for valence-conduction band electron promotion. This enhanced absorption corresponds to enhanced photocatalytic hydrogen evolution. Interestingly, with loading up to 1.75 mole%, the visible region absorption and H_2 production decreases (figure 6 and 7). Moreover, in the early stage, the 1.5 mole% Rh loading sample (figure 6) had a slightly higher activity than the 1.25 mole% Rh sample; however, the activity of the former system decreased gradually after 10 hours. This deactivation may imply the possibility of Rh acting as back-reaction sites. In order to reach the balance between recombination and generation of the electrons and holes, the distribution of Rh in the particles is very important. Indeed, aerogel synthesis can yield smaller particles than conventional solid-state synthesis methods. This smaller size can aid the electrons/holes to more rapidly to the particle surface because of a shorter travel distance. In other words, the generated excitons from one Rh will have a lower possibility of contacting another Rh on the path to the particle surface. Thus, the Rh loading is

critical, as is particle size. Moreover, figure 8 shows the TEM images of different $SrTiO_3$:Rh samples with different amounts of Rh. The areogel samples can have a very homogeneous particle size, which is only around 10 nm when the Rh loading was 1.0 mole% (figure 8a). However, a higher loading of Rh may cause the increase of particle size and a larger range of size distribution (figure 8d).

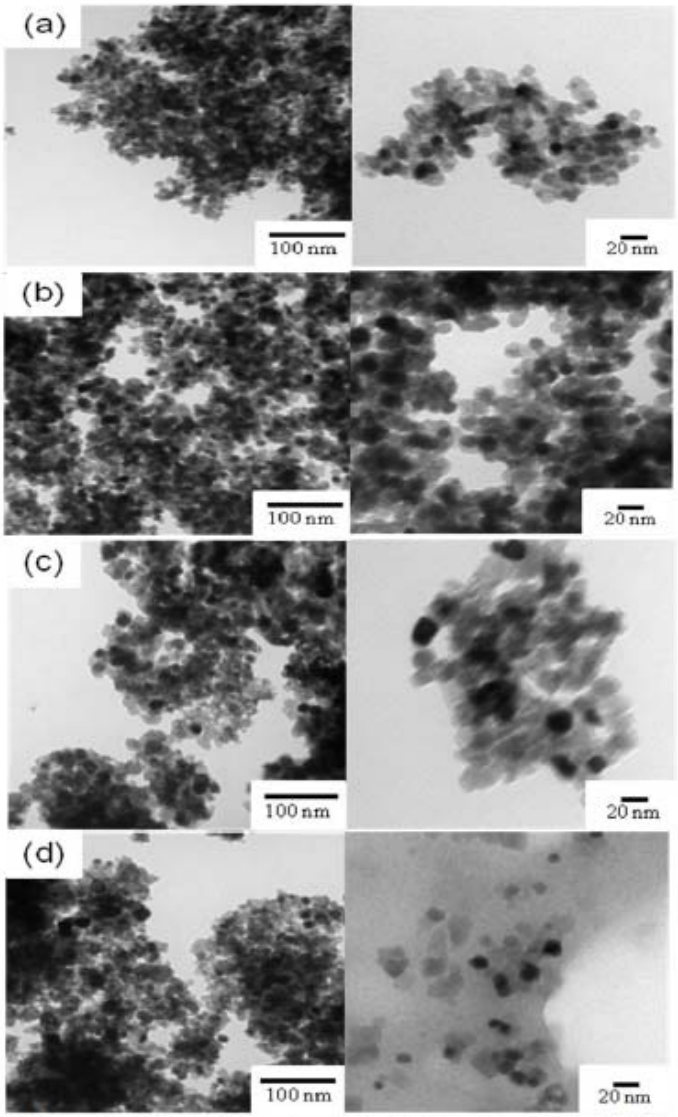

Figure 8. TEM images of Rh-doped aerogel synthesis $SrTiO_3$ (1.5 wt% Ru, cal. 500 °C) upon the different Rh doping amount (a) 1 mole% (b) 1.25 mole% (c) 1.5 mole% (d) 1.75 mole%

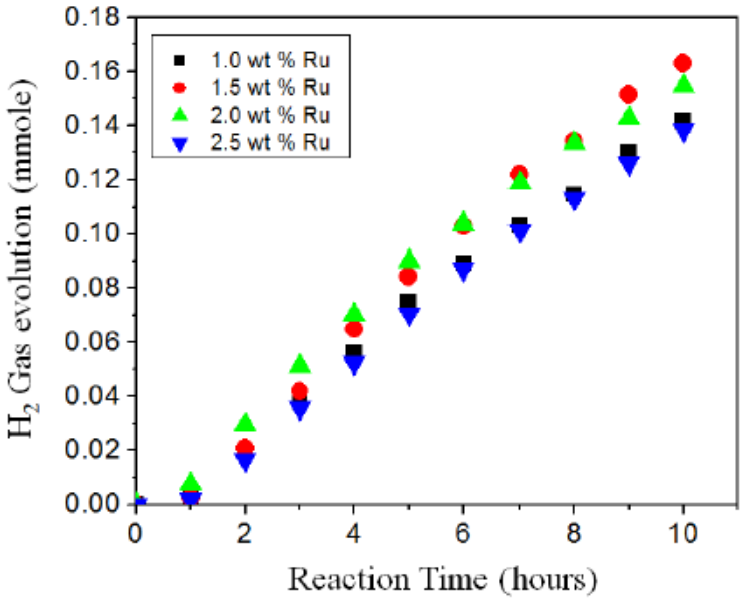

Figure 9. Dependence of H_2 evolution activity of aerogel $SrTiO_3$: Rh (1.25 mole % Rh, cal. 500 °C) upon different amounts of co-catalyst Ru in 10 vol % methanol solution (pH = 12.4, adjusted by NaOH) under visible light.

3.5. Dependence of H_2 evolution activity of aerogel Ru/$SrTiO_3$:Rh upon the different co-catalyst Ru amounts.

Figure 9 shows the dependence of H_2 evolution activity of aerogel $SrTiO_3$:Rh (1.25 mole %, cal. 500 ^oC) upon the different co-catalyst amounts. The optimal co-catalyst seems to be Ru/$SrTiO_3$:Rh(1.5 wt % Ru). Figure 9 shows that when the loading of Ru was more than 2.0 wt %, the photocatalyst had a high activity in the beginning but it changed to a lower rate after 5 hours. A possible explanation is similar to that discussed for Rh loading; too much Ru presence may lead to increased electron-hole pair recombination.

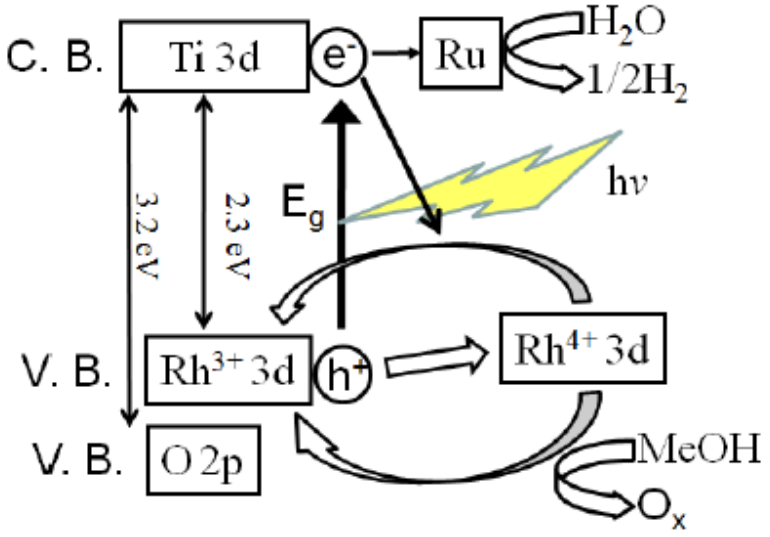

Figure 10. Proposed schematic diagram for visible light response of $Ru/SrTiO_3$:Rh photocatalyst.

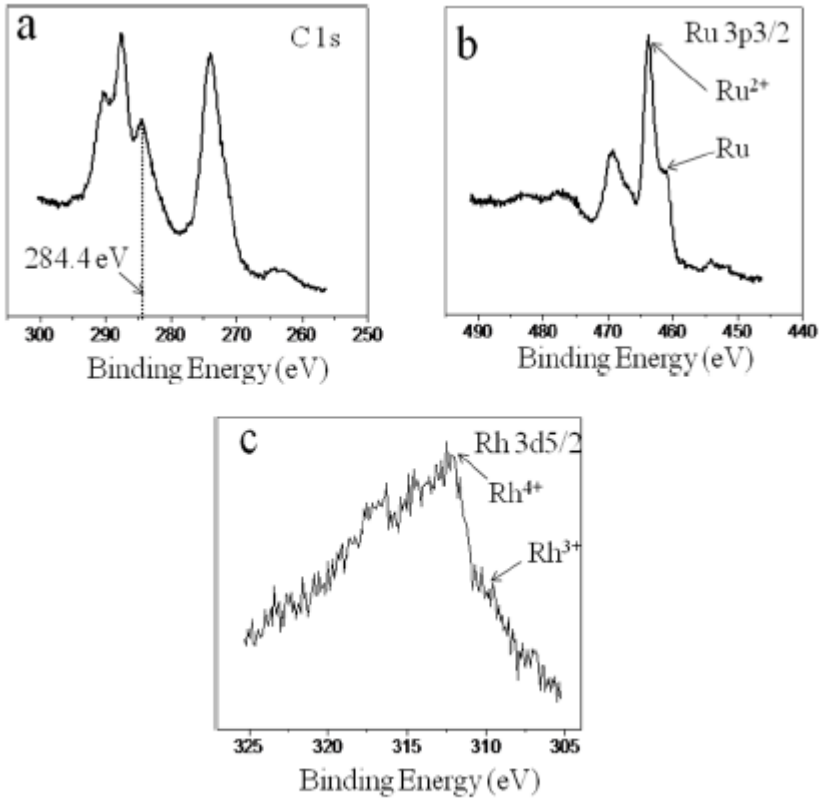

Figure 11. XPS spectra of $Ru/SrTiO_3$:Rh (1.25 mole % Rh, 1.5 wt% Ru, Cal. 500 °C) (a) C 1s (b) Ru 3p3/2 (c) Rh 3d5/2.

3.6. Mechanism.

The proposed schematic mechanism for the photocatalytic H_2 evolution on Ru/$SrTiO_3$:Rh is illustrated in figure 10. The visible light absorption bands in the diffuse reflectance spectrum are very likely due to Rh^{3+}. In figure 11c, The XPS data confirmed the presence of Rh^{3+} and Rh^{4+}. These Rh ions could be isolated or have neighbors, depending on loading, and what is needed is a balance favoring electron/hole formation and separation, rather than facilitating recombination. The Rh with higher oxidation number, such as Rh^{4+}, can be easily reduced back to Rh^{3+} by photogenerated electrons or by oxidizing methanol. The highly efficient H_2 evolution on the $SrTiO_3$:Rh photocatalyst under visible light irradiation indicates that Rh^{3+} works as an electron donor to the conduction band. It is the major electron pump for photocatalytic H_2 evolution. The electrons photogenerated in the conduction band transfer to Ru and reduce water to form H_2, while holes formed in the electron donor level oxidize methanol. The Ru may be present in oxidation states of 0 and 2+, which were observed by XPS (figure 11b). This indicates that the doped Rh^{3+} formed the visible light absorption center and the surface reaction center. Because of higher surface area, the optimum doping amount was 1.25%, which is higher than conventional solid-state synthesis samples.[15] During these experiments there was no O_2 evolution observed, even though the potential of generated holes might be thermodynamically high enough for oxidation of water to form O_2. However, there are no reaction centers for the four-electron oxidation for O_2 evolution. On the other hand, the standard redox potentials for HCHO/CH_3OH and H_2CO_3/CH_3OH are 0.232 and 0.044 V, so methanol oxidation is easy compared to O_2 evolution from water (1.23 V) from both thermodynamic and kinetic standpoints.[15] Moreover, it is well-known that O_2 evolution has a large overpotential (> 0.5 V).[15] Thus, it is clear that water oxidation is harder than methanol oxidation.

4. Conclusion

We have used a modified aerogel synthesis to prepare nanostructured high surface area Ru/$SrTiO_3$:Rh oxide photocatalysts that are active for H_2 evolution from an aqueous methanol solution under visible light irradiation. The aerogel method also provides for thin-film fabrication and increases possible applications. The visible light response was due to the transition from the electron donor level formed by Rh^{3+} ions to the conduction band composed of Ti 3d orbitals of $SrTiO_3$.[8] The absorption band in the visible light region from 400 nm to 520 nm directly corresponded to photocatalytic hydrogen evolution activity. The optimal synthesis condition is 1.25 mole % Rh, 1.5 wt % Ru, calcination temperature at 550 ^oC and pH = 12.4 aqueous methanol solution. The solution for hydrogen generation has to be basic (alkaline), which is unique from most other photocatalytic water splitting materials. The calcination temperature and dopant amount of Rh are two major factors that affect H_2 evolution.

Acknowlegment

We acknowledge the U.S. Marine Corp through M2 Corporation, and the NSF-EPSCoR Renewable Energy Project for financial support.

References

[1] Abe R, Takata T, Sugihara H and Domen K 2005 Photocatalytic overall water splitting under visible light by TaON and WO_3 with an IO^{3-}/I^- shuttle redox mediator *Chemical Communications* 3829-31

[2] Darwent J R and Mills A 1982 Photo-oxidation of water sensitized by WO_3 powder *Journal of the Chemical Society, Faraday Transactions 2: Molecular and Chemical Physics* **78** 359-67

[3] Demydov D and Klabunde K J 2004 Characterization of mixed metal oxides ($SrTiO_3$ and $BaTiO_3$) synthesized by a modified aerogel procedure *Journal of Non-Crystalline Solids* **350** 165-72

[4] Diao Y, Walawender W P, Sorensen C M, Klabunde K J and Ricker T 2001 Hydrolysis of Magnesium Methoxide. Effects of Toluene on Gel Structure and Gel Chemistry *Chemistry of Materials* **14** 362-8

[5] Fujihara K, Ohno T and Matsumura M 1998 Splitting of water by electrochemical combination of two photocatalytic reactions on TiO_2 particles *Journal of the Chemical Society, Faraday Transactions* **94** 3705-9

[6] Kato H, Hori M, Konta R, Shimodaira Y and Kudo A 2004 Construction of Z-scheme type heterogeneous photocatalysis systems for water splitting into H_2 and O_2 under visible light irradiation *Chem. Lett.* **33** 1348-9

[7] Kato H, Sasaki Y, Iwase A and Kudo A 2007 Role of Iron Ion Electron Mediator on Photocatalytic Overall Water Splitting under Visible Light Irradiation Using Z-Scheme Systems *Bulletin of the Chemical Society of Japan* **80** 2457-64

[8] Konta R, Ishii T, Kato H and Kudo A 2004 Photocatalytic Activities of Noble Metal Ion Doped $SrTiO_3$ under Visible Light Irradiation. In: *The Journal of Physical Chemistry B*: American Chemical Society) pp 8992-5

[9] Kudo A, Omori K and Kato H 1999 A Novel Aqueous Process for Preparation of Crystal Form-Controlled and Highly Crystalline $BiVO_4$ Powder from Layered Vanadates at Room Temperature and Its Photocatalytic and Photophysical Properties *Journal of the American Chemical Society* **121** 11459-67

[10] Lee Y, Terashima H, Shimodaira Y, Teramura K, Hara M, Kobayashi H, Domen K and Yashima M 2007 Zinc Germanium Oxynitride as a Photocatalyst for Overall Water Splitting under Visible Light *The Journal of Physical Chemistry C* **111** 1042-8

[11] Maeda K, Takata T, Hara M, Saito N, Inoue Y, Kobayashi H and Domen K 2005 GaN:ZnO Solid Solution as a Photocatalyst for Visible-Light-Driven Overall Water Splitting *Journal of the American Chemical Society* **127** 8286-7

[12] Maeda K, Teramura K, Lu D, Takata T, Saito N, Inoue Y and Domen K 2006 Photocatalyst releasing hydrogen from water *Nature* **440** 295-

[13] Rabuffetti F A, Stair P C and Poeppelmeier K R 2010 Synthesis-Dependent Surface Acidity and Structure of $SrTiO_3$ Nanoparticles *The Journal of Physical Chemistry C* **114** 11056-67

[14] Sasaki Y, Iwase A, Kato H and Kudo A 2008 The effect of co-catalyst for Z-scheme photocatalysis systems with an Fe^{3+}/Fe^{2+} electron mediator on overall water splitting under visible light irradiation *Journal of Catalysis* **259** 133-7

[15] Sasaki Y, Nemoto H, Saito K and Kudo A 2009 Solar Water Splitting Using Powdered Photocatalysts Driven by Z-Schematic Interparticle Electron Transfer without an Electron Mediator *The Journal of Physical Chemistry C* **113** 17536-42

[16] Sayama K, Mukasa K, Abe R, Abe Y and Arakawa H 2001 Stoichiometric water splitting into H and O using a mixture of two different photocatalysts and an IO^{3-}/I^{-} shuttle redox mediator under visible light irradiation *Chemical Communications* 2416-7
[17] Shimodaira Y, Kato H, Kobayashi H and Kudo A 2006 Photophysical Properties and Photocatalytic Activities of Bismuth Molybdates under Visible Light Irradiation *The Journal of Physical Chemistry B* **110** 17790-7
[18] Utamapanya S, Klabunde K J and Schlup J R 1991 Nanoscale metal oxide particles/clusters as chemical reagents. Synthesis and properties of ultrahigh surface area magnesium hydroxide and magnesium oxide *Chemistry of Materials* **3** 175-81